

## Pressure, Surface Tension, and Dripping of Self-Trapped Laser Beams

David Novoa, Humberto Michinel, and Daniele Tommasini

*Departamento de Física Aplicada, Faculdade de Ciências de Ourense, Universidade de Vigo, As Lagoas s/n, Ourense, ES-32004 Spain*  
(Received 25 March 2009; published 10 July 2009)

We show that a laser beam which propagates through an optical medium with Kerr (focusing) and higher order (defocusing) nonlinearities displays pressure and surface-tension properties yielding capillarity and dripping effects totally analogous to usual liquid droplets. The system is reinterpreted in terms of a thermodynamic grand potential, allowing for the computation of the pressure and surface tension beyond the usual hydrodynamical approach based on Madelung transformation and the analogy with the Euler equation. We then show both analytically and numerically that the stationary soliton states of such a light system satisfy the Young-Laplace equation and that the dynamical evolution through a capillary is described by the same law that governs the growth of droplets in an ordinary liquid system.

DOI: 10.1103/PhysRevLett.103.023903

PACS numbers: 42.65.Tg, 03.75.Lm, 42.65.Jx

*Introduction.*—Since the pioneering paper of Piekara in the 1970s [1], many works have highlighted the interesting properties of laser beams whose propagation is described by the so-called cubic-quintic (CQ) nonlinear Schrödinger equation (NLSE) with competing nonlinearities. Cavitation, superfluidity, and coalescence have been investigated [2,3] in the context of liquid He, where the model is a simple approach which does not take into account nonlocal interactions. Stable optical vortex solitons and the existence of top-flat states have also been reported in materials with CQ optical susceptibility [4]. Recent experiments about filamentation of high-power laser pulses have shown that the CQ regime could be achievable in CS<sub>2</sub> [5] as well as in some chalcogenide glasses [6]. Theoretical calculations suggest that atomic coherence may be used to induce a giant CQ-like refractive index in a Rb gas [7].

On the other hand, this model has been shown to display surface properties in numerical simulations of soliton collisions [8] that have been considered as a trace of a liquid state of light [7,9]. Here, we will provide the first analytical, quantitative demonstration of the liquid behavior of the system in 2 + 1 dimensions, both in its stationary soliton solutions and in the dynamical evolution when a light bump is forced to pass through a waveguide simulating a capillary. In particular, we will provide the first consistent computation of the pressure and surface tension of self-trapped light beams in 2 + 1 dimensions, and show both analytically and numerically that they satisfy the Young-Laplace (YL) equation that gives the equilibrium of usual droplets. Subsequently, we will demonstrate that the system dripping properties are governed by the same generalized YL that applies to an ordinary liquid. These results show the deep connection between the nonlinear dynamics of laser beams and coherent liquids at zero temperature [10].

*Thermodynamic model.*—We will consider the paraxial propagation through an ideal CQ medium of a linearly polarized laser beam, whose complex amplitude distribu-

tion  $\Psi$  is described by the nonlinear Schrödinger equation

$$i \frac{\partial \Psi}{\partial z} + \frac{1}{2} \nabla_{\perp}^2 \Psi + \gamma |\Psi|^2 \Psi - \delta |\Psi|^4 \Psi = 0, \quad (1)$$

where  $z$  is the propagation distance multiplied by  $2\pi/\lambda$  and  $\lambda$  is the wavelength of the continuous light beam,  $\nabla_{\perp}^2$  is the transverse Laplace operator in terms of  $x, y$ , the spatial variables multiplied by  $2\pi\sqrt{2n_0}/\lambda$ , where  $n_0$  is the linear refractive index of the medium,  $\gamma$  and  $\delta$  are proportional to the (opposite)  $\chi^{(3)}$  and  $\chi^{(5)}$  optical susceptibilities, respectively.

It is well known that the stationary version of Eq. (1) admits localized solitonlike solutions [1] of the form  $\Psi_A(x, y, z) = A(x, y)e^{-i\mu z}$ , where  $\mu$  is the propagation constant. In particular, it has been shown numerically that high-power solitons feature top-flat profiles [4]. These modes can only be calculated numerically and coexist with plane waves solutions of constant amplitude  $\Psi_A(x, y, z) = Ae^{-i\mu z}$ , which lead by substitution in Eq. (1) to  $\mu = \delta|A|^4 - \gamma|A|^2$ . The existence domain for solitons is  $\mu \in (\mu_{\infty}, 0)$ , where  $\mu_{\infty} = -\frac{3\gamma^2}{16\delta}$ .

As discussed in [11], the stationary solutions of Eq. (1) can be derived from a variational principle  $\frac{\delta \Omega}{\delta \Psi^*} = 0$  from Landau's grand potential  $\Omega = H - \mu N$ , where  $H$  is the Hamiltonian,  $N = \int |\Psi|^2 dS$  the particle number (in our system the photon flux through the transverse section  $S$ ), and  $\mu$  the chemical potential. In fact, the identification of the latter with the propagation constant that we have defined above ensures that  $\Omega$  coincides (up to a sign choice) with the Lagrangian, yielding

$$\Omega = \int \left[ \frac{1}{2} |\nabla_{\perp} \Psi|^2 - \frac{\gamma}{2} |\Psi|^4 + \frac{\delta}{3} |\Psi|^6 - \mu |\Psi|^2 \right] dS. \quad (2)$$

In three-dimensional systems, the partial derivative of  $\Omega$  with respect to the volume at constant chemical potential and temperature would give minus the pressure  $p$ . For our

2D model at zero temperature, it is then natural to use the derivative with respect to the area  $S$ ,

$$p = -(\partial\Omega/\partial S)_\mu \\ = -\frac{1}{2}|\nabla_\perp\Psi|^2 + \frac{\gamma}{2}|\Psi|^4 - \frac{\delta}{3}|\Psi|^6 + \mu|\Psi|^2. \quad (3)$$

In Fig. 1 we plot an example of a “flattop” stationary state, corresponding to  $\mu/\mu_\infty = 0.98$ , together with its pressure distribution. For all this type of solutions, in the wide flat region the value of the pressure is positive and equal to the central value  $p(0) \equiv p_c$ . This behavior contrasts with that for the low amplitude, quasi-Gaussian solitons, whose pressure distribution does not display a top-flat central region. On the other hand, the beam amplitude of the top-flat solitons close to the origin can be straightforwardly obtained as

$$|A(0,0)|^2 = \frac{\gamma}{2\delta} + \frac{\sqrt{\gamma^2 + 4\delta\mu}}{2\delta}, \quad (4)$$

which yields for the pressure at the center of the beam ( $p_c$ ) the following analytical expression:

$$p_c = \frac{(\gamma + \sqrt{\gamma^2 + 4\delta\mu})^2(-\gamma + 2\sqrt{\gamma^2 + 4\delta\mu})}{24\delta^2}. \quad (5)$$

Notice that  $p_c$  vanishes at the limits of the existence domain:  $\mu = 0$  (trivial zero-amplitude solution) and  $\mu = \mu_\infty$  (infinite flattop with  $|A_\infty|^2 = 0.75\gamma/\delta$ ).

*Limitations of the hydrodynamical analogy.*—Our present purpose is to use the previous formalism in order to study the physical properties of the system. First, let us try to apply the commonly used hydrodynamical analogy, based on introducing the so-called Madelung transformation [12]  $\psi = \rho^{1/2}e^{i\phi}$ , where  $\rho$  is a positive definite real function and  $\phi$  is a real phase, eventually depending on the variables  $x$ ,  $y$ , and  $z$ . After substituting in Eq. (1), and

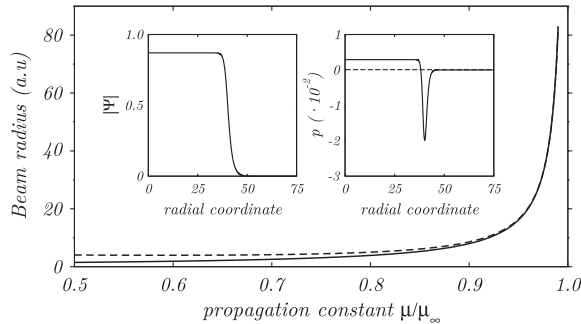


FIG. 1. Plot of radius versus propagation constant for different localized stationary solutions of Eq. (1). Solid (dashed) line corresponds to numerical (analytical) calculations. The left (right) inner picture shows the field modulus profile (pressure distribution) of a stationary beam with  $\mu/\mu_\infty = 0.98$ . Notice that close to the origin the homogeneous pressure is positive, whereas in the inhomogeneous region it becomes negative. Beam radius is represented in adimensional units.

separating both the real and the imaginary part, we get two equations. The first one is a continuity equation, that is used to establish an analogy with hydrodynamics and to identify  $\nabla\phi$  with a current, i.e., a velocity field  $\mathbf{v}$ . The second equation is

$$\frac{\partial\mathbf{v}}{\partial z} + \nabla_\perp\left(\frac{\mathbf{v}^2}{2} + \frac{1}{2\rho^{1/2}}\nabla_\perp^2\rho^{1/2} + \gamma\rho - \delta\rho^2\right) = 0. \quad (6)$$

Here, the usual approach [2] is to assume that the term  $\frac{1}{2\rho^{1/2}}\nabla_\perp^2\rho^{1/2}$  can be neglected. In this case, Eq. (6) is identical to the known Euler equation of hydrodynamics provided that  $\nabla_\perp(\gamma\rho - \delta\rho^2) = -\frac{\nabla_\perp p}{\rho}$ . This formula was used, e.g., in Ref. [2] in order to derive an expression for the pressure of the homogenous phase, which coincides with our result of Eq. (5) for the top-flat region of the solitons. One could hope that this analogy could be generalized also to the nonhomogenous zones, such as that corresponding to values of the radial coordinate  $r$  around the radius  $R$  of the beam. However, we will see that this is not the case. For a (nonrotational) top-flat soliton the phase term is simply equal to  $\phi = -\mu z$ , therefore  $\mathbf{v} = \nabla_\perp\phi = 0$ . Note that  $\mu$  is the propagation constant which is just a constant number for the given soliton. Therefore, by substituting in Eq. (6), we get

$$\nabla_\perp\left(\frac{1}{2\rho^{1/2}}\nabla_\perp^2\rho^{1/2} + \gamma\rho - \delta\rho^2\right) = 0. \quad (7)$$

In other words, in this case the term that is usually neglected is *exactly* equal and opposite to the part that is used to compute the pressure. Therefore, neglecting such a term would correspond to a 100% error. In fact, for any soliton solution, having  $\mathbf{v} = 0$ , Euler equation would unavoidably imply a constant pressure, which cannot be the case in any region where the spatial variation of the density is important. Nevertheless, in spite of this failure of the ordinary hydrodynamical approach, we will see that the “pressure” distribution in the nonhomogeneous region can still be given a deep physical interpretation.

*Equilibrium and surface tension.*—Figure 1 suggests that the  $\Omega$  potential, as given by the spatial integral of  $-p$ , can be written as the sum of two contributions: one from the top-flat region, which is  $-\pi R^2 p_c$  with a good accuracy, and another from the region near the border, where the field is spatially dependent, which is  $-2\pi\int_R^\infty rp(r)dr$ . Thus, we get the following analytical approximation for the  $\Omega$  potential of the flattop solutions:

$$\Omega \simeq -\pi R^2 p_c + 2\pi\sigma R, \quad (8)$$

where we have defined a parameter  $\sigma \equiv -\frac{1}{R}\int_R^\infty rp(r)dr$ . We will now argue on how  $\sigma$  can be identified with the surface tension of the light beam. In the first place, we have computed numerically the parameter  $\sigma$  for the different high-power top-flat solitons, and we have found that it converges quickly to a fixed value  $\sigma \simeq 0.057$  as soon as

$|\mu|$  approaches the limiting value  $\mu_\infty$ . In such a limit, the central pressure goes to zero and the only important contribution to the integral defining  $\sigma$  comes from the gradient term of Eq. (3). Thus  $\sigma \simeq -\frac{1}{2R} \int_R^\infty r |\nabla_\perp \Psi|^2 dr$ .

We can then get an analytical approximation for  $\sigma$  by noting that for large  $R$  and  $r$ ,  $\nabla_\perp \Psi \simeq d\Psi/dr$ , and the multiplying  $r$  in the integrand can be approximated by  $R$  in the comparatively thin “surface” region. Taking into account that for large  $r$  Eq. (1) yields  $A'(r)^2 \simeq -\gamma A(r)^4/2 + \delta A(r)^6/3 + \mu A(r)^2$ , and substituting the limiting value  $\mu \rightarrow \mu_\infty = -\frac{3\gamma^2}{16\delta}$ , we get

$$\sigma \simeq \frac{9\gamma^2}{64\sqrt{6}\delta^{3/2}}. \quad (9)$$

For instance, the choice  $\gamma = \delta = 1$  gives  $\sigma = 0.057$ , in complete agreement with our numerical value. From Eq. (8), taking into account that  $\sigma$  is constant, we get

$$\frac{d\Omega}{dR} \simeq -\pi \left[ \frac{d(R^2 p_c)}{dR} - 2\sigma \right]. \quad (10)$$

Our numerical calculations show that the growth in  $R$  holds the thermodynamical equilibrium (i.e.,  $\frac{d\Omega}{dR} \simeq 0$ ), within a relative error which turns out to be as small as  $\frac{d\Omega}{dR} < 10^{-4} \frac{\Omega}{R}$  for all the range of flattop eigenmodes considered. Therefore, we can set  $\frac{d\Omega}{dR} = 0$  in Eq. (10), and we get  $\frac{d(R^2 p_c)}{dR} = 2\sigma$ , or

$$p_c = 2 \frac{\sigma}{R}, \quad (11)$$

which is the celebrated Young-Laplace equation [13] for spherical liquid droplets being  $\sigma$  the surface tension of the system. Therefore, despite the failure of the usual hydrodynamic approach, we have demonstrated that the pressure distribution in the inhomogeneous region has a deep physical interpretation. In fact, the integral of the pressure in the nonhomogeneous surface region gives the surface tension ( $\sigma$ ), i.e., the inward force that compensates the outward positive inner force described by the pressure  $p_c$ , in order to keep the droplet stationary.

Instead of directly comparing Eq. (11) with the numerical simulation, we will equivalently test the inverted equation  $R = 2\sigma/p_c$ , where  $p_c$  can be expressed analytically in terms of either the central amplitude  $A$  or of the propagation constant  $\mu$ , by using Eqs. (5) and (9). This result provides the first analytical expression for the radius  $R$  of the bidimensional top-flat solitons as a function, e.g., of  $\mu$ , and is compared with the numerical solutions of the stationary version of Eq. (1) in Fig. 1. As it can be appreciated in the figure, the agreement between the analytical formula and the numerical computation is remarkable, and becomes complete when  $|\mu|$  approaches  $|\mu_\infty|$ . This result confirms our theoretical framework and provides the first formal demonstration, by validation of the YL equation, of the liquid properties of the flattop solutions in the (2 + 1)-

dimensional CQ model. Moreover, from Eq. (11) it can be inferred that, as  $R \rightarrow \infty$ , the value of  $p_c$  vanishes, indicating that surface-tension effects are not needed to balance the inner pressure, as it is the case of standard liquids described by the YL equation.

*Dripping of light droplets.*—In classical fluid mechanics, the presence of surface-tension effects can be appreciated in the dynamical phenomenon of capillarity [13,14]. Here, in order to study droplets formation and dripping in our system, we have introduced in Eq. (1) an external “channel-type” linear optical waveguide  $V(x, y)$ , superposed to the CQ nonlinearity. This waveguiding structure consists of three regions with indices  $n_1 = 0.002$  (top),  $n_2 = 0.0028$  [channel filled up in dark (brown) and bottom zone], and  $n_3 = 0.001$  (rectangular zones flanking the channel), as can be seen in Fig. 2(a). In our simulations, we compare the evolution of two initial eigenstate beams with propagation constants  $\mu/\mu_\infty = 0.01$  [quasi-Gaussian beam of Fig. 2(a)] and  $\mu/\mu_\infty = 0.98$  [flattop beam of Fig. 2(d)], both located within the waveguide top region. Depending on the channel size, and keeping  $n_3 < n_2, n_1$ , above a given value of  $\Delta n = n_2 - n_1$  in both cases a significant amount of beam power starts to flow from the initial eigenstate through the channel, as shown in Figs. 2(b) and 2(e). It is noteworthy that the light stream inside the channel does not suffer any destabilization and remains connected to the initial source of light; i.e., the guide prevents the appearance of modulational instability. At the output of the channel, it can be seen in Fig. 2(c) that the low-power distribution spreads like a (coherent) gas in free expansion. This lack of liquidlike behavior corresponds to the fact that these solutions do not obey the

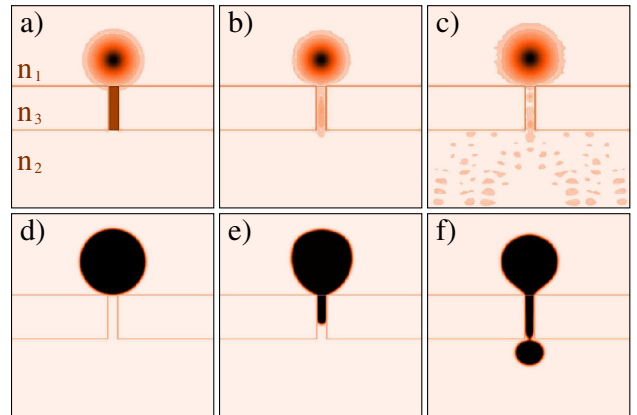


FIG. 2 (color online). Simulation of the modulus evolution of two different types of beams. The upper row shows a Gaussian profile with low power, corresponding to a “photonic gas,” whereas the lower row displays the propagation of a high-power flattop state yielding to liquidlike behavior (dripping). The size of all pictures is  $x, y \in [-250, 250]$  in adimensional units. The propagation distances in (a)–(d), (b)–(e), (f), and (c) are respectively  $z = 0, 11\,000, 27\,000, 45\,000$ . The refractive index structure indicated in (a) is the same in all snapshots.

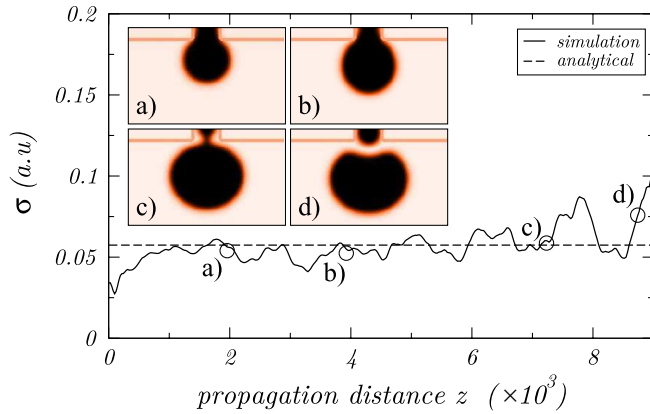


FIG. 3 (color online). Numerically calculated values of the surface tension along the droplet-formation process. Solid (dashed) line corresponds to numerical (analytical) calculations of  $\sigma$ . Insets: Snapshots showing different stages of evolution of the light droplet for different values of  $z$ . Circles in the figure refer to upper insets. The spatial scales spanned are  $x \in [-50, 50]$ ,  $y \in [-20, -80]$ .  $\sigma$  is represented in adimensional units.

YL equation. However, the light flowing from the flattop beam yields to the formation of a droplet, as can be appreciated in Fig. 2(f) and in the insets of Fig. 3.

As it can be observed in the insets of Fig. 3, before the release of the droplet, the end of the light stream becomes narrower as in the case of usual liquids falling from a tap [15]. In fact, all the steps in Fig. 2 are qualitatively very similar to those obtained both in real experiments and in simulations with liquids [14–17].

Finally, we have also performed a *quantitative* test by comparing the numerical simulation with the generalized YL equation that describes the growth of an elliptic bubble of an ordinary liquid system,  $p_c = \sigma(\frac{1}{R_I} + \frac{1}{R_{II}})$ , where  $R_I$  and  $R_{II}$  are the principal radii [13]. In Fig. 3, we have plotted the quantity  $\sigma = p_c / (\frac{1}{R_I} + \frac{1}{R_{II}})$  for the “dripping” simulation of Fig. 2 at several propagation distances, assuming  $z = 0$  where the light droplet first appears. We see that the numerical value of  $\sigma$  oscillates around the same value that we have calculated analytically in Eq. (9) for the stationary solutions. This demonstrates that the droplets are formed close to stationary equilibrium, and they grow according to the generalized YL equation as in the case of an ordinary liquid.

*Conclusions.*—We have provided the first consistent computation of the pressure distribution and surface tension of solitons appearing in the propagation of self-trapped laser beams described by the  $(2 + 1)$ -dimensional CQ NLSE, and we have shown both analytically and numerically that they satisfy the Young-Laplace equation that governs the equilibrium of usual liquid droplets. Subsequently, we have also demonstrated that the system dripping properties are governed by the same generalized

YL that applies to an ordinary liquid. As far as we know, this is the first explicit example of a coherent fluid showing capillarity.

Our general approach also applies to other physical systems like atomic Bose-Einstein condensates. In particular, our new analysis on the limitations of the universally used Madelung hydrodynamical approach can also be applied to many different nonlinear systems modeled by NLS-type equations. These results open the door to the demonstration of a new type of phase transitions at zero temperature, which are not ruled by quantum fluctuations but induced from purely nonlinear effects, and to the realization of experiments not only in nonlinear optics but also in the field of quantum fluids.

We thank A. Ferrando for useful discussions and support by MICIIN, Spain (projects FIS2006-04190 and FIS2007-62560) and Xunta de Galicia [project PGIDIT04TIC383001PR and (D.N.) grant from Consellería de Innovación e Industria-Xunta de Galicia].

- [1] A. H. Piekara, J. S. Moore, and M. S. Feld, *Phys. Rev. A* **9**, 1403 (1974).
- [2] C. Josserand, Y. Pomeau, and S. Rica, *Phys. Rev. Lett.* **75**, 3150 (1995).
- [3] C. Josserand and S. Rica, *Phys. Rev. Lett.* **78**, 1215 (1997).
- [4] M. Quiroga-Teixeiro and H. Michinel, *J. Opt. Soc. Am. B* **14**, 2004 (1997); D. Mihalache *et al.*, *Phys. Rev. Lett.* **88**, 073902 (2002).
- [5] M. Centurion, Ye Pu, M. Tsang, and D. Psaltis, *Phys. Rev. A* **71**, 063811 (2005).
- [6] F. Smektala, C. Quemard, V. Couderc, and A. Barthelemy, *J. Non-Cryst. Solids* **274**, 232 (2000).
- [7] H. Michinel, M. J. Paz-Alonso, and V. M. Pérez-García, *Phys. Rev. Lett.* **96**, 023903 (2006); A. Alexandrescu, H. Michinel, and V. M. Pérez-García, *Phys. Rev. A* **79**, 013833 (2009).
- [8] D. E. Edmundson and R. H. Enns, *Phys. Rev. A* **51**, 2491 (1995); M. J. Paz-Alonso, D. Olivieri, H. Michinel, and J. R. Salgueiro, *Phys. Rev. E* **69**, 056601 (2004).
- [9] H. Michinel, J. Campo-Táboas, R. García-Fernández, J. R. Salgueiro, and M. L. Quiroga-Teixeiro, *Phys. Rev. E* **65**, 066604 (2002).
- [10] R. Y. Chiao, *Opt. Commun.* **179**, 157 (2000); R. Y. Chiao *et al.*, *J. Phys. B* **37**, S81 (2004); R. Y. Chiao *et al.*, *Phys. Rev. A* **69**, 063816 (2004).
- [11] D. Novoa *et al.*, *Physica (Amsterdam)* **238D**, 1490 (2009).
- [12] E. Madelung, *Die Mathematischen Hilfsmittel des Physikers* (Springer-Verlag, Berlin, 1957).
- [13] L. D. Landau and E. M. Lifshitz, *Fluid Mechanics* (Pergamon, Oxford, 1984).
- [14] J. Eggers, *Rev. Mod. Phys.* **69**, 865 (1997).
- [15] V. Grubelnik and M. Marhl, *Am. J. Phys.* **73**, 415 (2005).
- [16] R. Suryo and O. A. Basaran, *Phys. Rev. Lett.* **96**, 034504 (2006).
- [17] O. E. Yildirim, Q. Xu, and O. A. Basaran, *Phys. Fluids* **17**, 062107 (2005).